

Nanocomposites of Nitrogen-Doped Carbon Dots/Hydrotalcite with Enhanced Solid-State Fluorescence for Recognition of Latent Fingerprints

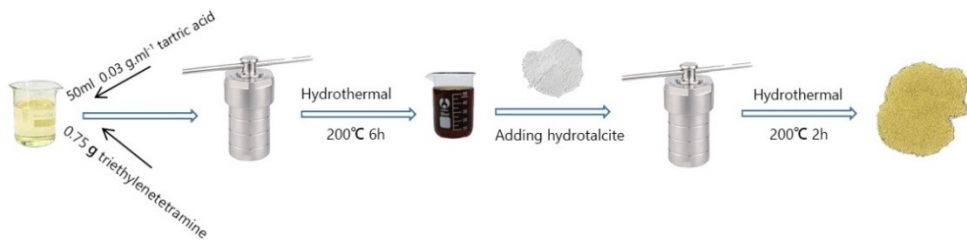
Da-Wu Li^{1,2,#}, Xing-Fu Zhang^{3,#}, Xiao-Tong Zhang³, Xiao-Sen lv^{1,2,*}, Nan You^{3,*}

(1. College of Forensic Science, Criminal Investigation Police University of China, Shenyang, Liaoning, 110035, China; 2. Key Laboratory of Impression Evidence Examination and Identification Technology, Ministry of Public Security, Shenyang, Liaoning, 110035, China; 3. College of Petrochemical Engineering, Liaoning Petrochemical University, Fushun, 113001)

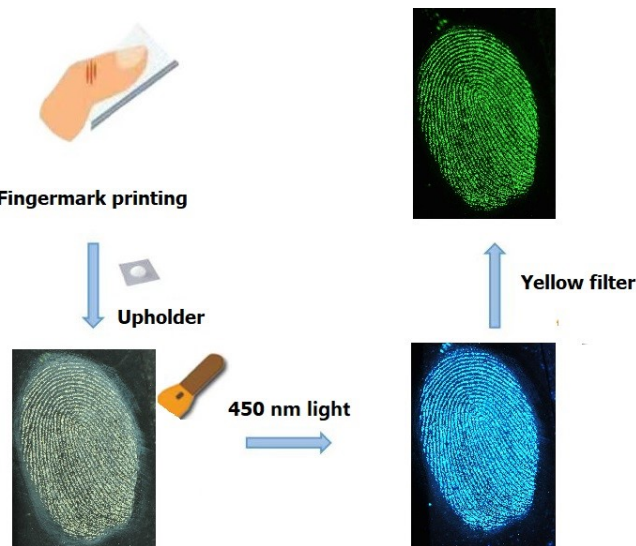
Email: lvxiaosen@126.com (X-S lv) and younan_77@163.com (N You)

Characterization

The surface morphology of the as-prepared product was observed by a transmission electron microscope (FEI Tecnai G2 20, USA) and scanning electron microscope (Shimadzu SS 550) equipped with an energy-dispersive X-ray analyzer. The crystalline characteristics of the as-prepared product underwent X-ray diffraction analysis using a Bruke Model AXS D8 ADVANCE X-ray diffractometer from 2θ of 5–80° with 0.01° scan step. The fluorescence spectral measurements were carried out using a Hitachi F-4500 fluorescence spectrometer.



Scheme S1 A schematic diagram of the N-CDs@hydrotalcite synthesis



Scheme S2 General process for the identification of the LFPs.

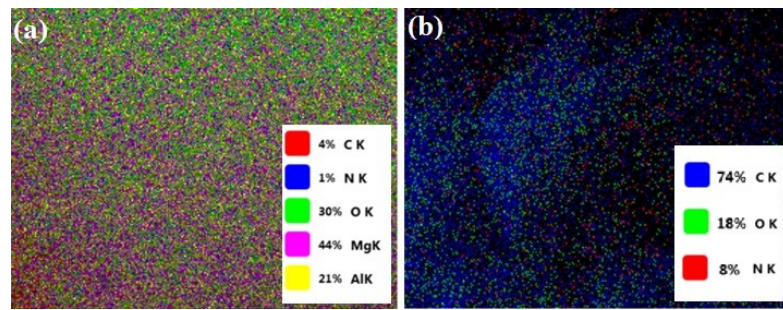


Figure S1 EDS spectrum of the N-CD/hydrotalcite

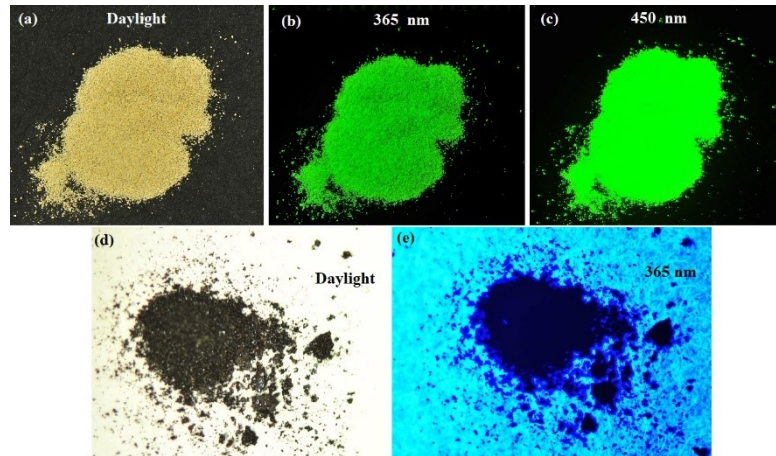


Figure S2 Appearance of the N-CD/hydrotalcite in daylight (a), and under irradiation with 365 nm UV-light (b) and 450 nm light (c).

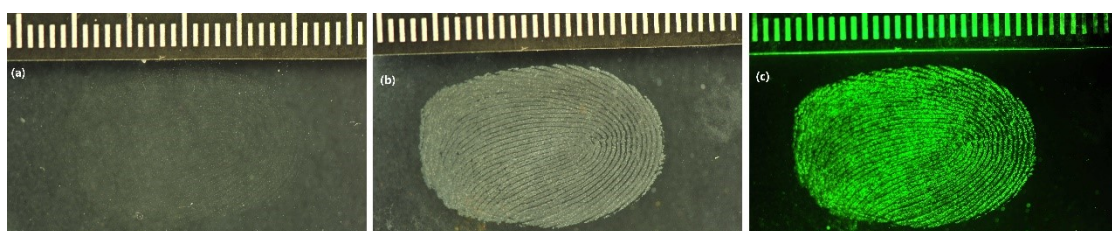


Figure S3 The images of LFPs on glass slide (a) before development, (b) after development using N-CD/hydrotalcite, and (c) under 450 nm light.

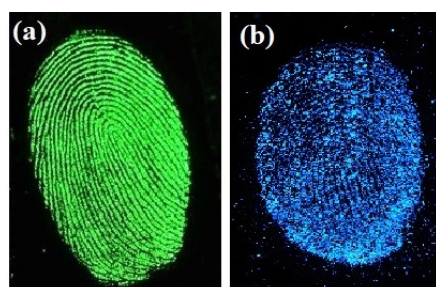


Figure S4 Fluorescent images of the LFPs developed by the (a) N-CD/hydrotalcite and (b) N-CD nanoparticles on glass slide under 450 nm light.

Table S1 Statistical table of ridge, Furrow and sweat hole size

Number	Ridge/mm	Furrow/mm	Sweat pore length/mm	Distance of sweat pore/mm
1	0.253	0.165	0.089	0.334
2	0.246	0.124	0.088	0.345
3	0.2067	0.097	0.108	0.41
4	0.218	0.077	0.11	0.326
5	0.24	0.097	0.056	0.359
6	0.201	0.148	0.093	0.359
7	0.184	0.073	0.059	0.256
8	0.146	0.097	0.039	0.368
9	0.162	0.121	0.039	0.41
10	0.18	0.048	0.056	0.379
11	0.18	0.124	0.077	0.35
12	0.197	0.124	0.064	0.41
13	0.218	0.097	0.114	0.32
14	0.265	0.087	0.09	0.245
15	0.265	0.121	0.128	0.36
16	0.264	0.124	0.077	0.416
17	0.247	0.077	0.149	0.325
18	0.194	0.1	0.083	0.315
19	0.194	0.148	0.1	0.376
20	0.232	0.124	0.06	0.31
21	0.247	0.097	0.056	0.21
22	0.27	0.073	0.06	0.334
23	0.201	0.077	0.083	0.265
24	0.257	0.097	0.073	0.325
25	0.24	0.131	0.122	0.384
26	0.262	0.073	0.065	0.308
27	0.201	0.124	0.108	0.297
28	0.201	0.097	0.066	0.42
29	0.218	0.073	0.089	0.409
30	0.285	0.21	0.064	0.5
31	0.279	0.26	0.07	0.274
32	0.253	0.135	0.046	0.339
33	0.285	0.24	0.07	0.43
34	0.269	0.21	0.059	0.4
35	0.286	0.135	0.06	0.51
Max	0.286	0.21	0.14	0.51
Min	0.180	0.073	0.05	0.21
Average	0.23	0.12	0.08	0.35

